Copy 4
RM L58C27

C.2

NACA RM L58C27

RESEARCH MEMORANDUM

INVESTIGATION OF THE AERODYNAMIC CHARACTERISTICS OF A MODEL OF A SUPERSONIC BOMBER CONFIGURATION WITH A SWEPT AND AN UNSWEPT WING AT MACH NUMBERS FROM 1.79 TO 2.67

By H. Norman Silvers and Raymond L. Zedekar

Langley Aeronautical Laboratory
Langley Field, Va.

NATIONAL ADVISORY COMMITTEE FOR AERONAUTICS

WASHINGTON

July 21, 1958

NATIONAL ADVISORY COMMITTEE FOR AERONAUTICS

RESEARCH MEMORANDUM

INVESTIGATION OF THE AERODYNAMIC CHARACTERISTICS OF A MODEL OF A SUPERSONIC BOMBER CONFIGURATION WITH A SWEPT AND AN UNSWEPT WING AT MACH NUMBERS FROM 1.79 TO 2.67*

By H. Norman Silvers and Raymond L. Zedekar

SUMMARY

The investigation was made in the Langley Unitary Plan wind tunnel at Mach numbers of 1.79 to 2.67 on a wing-fuselage combination and on the wing-fuselage combination with a complete tail configuration. Two wing plan forms were investigated on the fuselage. Both plan forms were of aspect ratio 3.20; one had 45.0° sweepback of the quarter-chord line and a taper ratio of 0.20 and the other had 19.2° sweepback of the quarter-chord line and a taper ratio of 0.40. The 45.0° swept wing had NACA 64A204.5 airfoil sections and the 19.2° swept wing had 3.5-percent-thick circular-arc airfoil sections.

The results showed that the lift-curve slope of the wing-fuselage combination with the 19.2° swept wing was higher than with the 45.0° swept wing, and the minimum drag coefficient was 0.0040 lower than that for the 45.0° swept wing probably due to the thinner airfoil section. The drag-due-to-lift factor was essentially the same for both wing plan forms. The determination of the lateral stability characteristics of the model with the complete tail and the 19.2° swept wing, made at a Mach number of 2.18 and an angle of attack of -2.5°, indicated that the model was directionally stable.

INTRODUCTION

Tests have been made in the Langley Unitary Plan wind tunnel as a part of a continuing research effort on bomber configurations intended to operate at supersonic speeds. These tests were made to determine the longitudinal aerodynamic characteristics of wing-fuselage combinations with the two different wing plan forms at Mach numbers from 1.79

*Title, Unclassified.

to 2.67. In addition, the lateral stability characteristics of one of the combinations were obtained with complete tail assembly at a Mach number of 2.18 and an angle of attack of -2.5°.

The results of this investigation are presented herein without analysis.

COEFFICIENTS AND SYMBOLS

Force and moment coefficients are referred to the stability system of axes as illustrated in figure 1. The moments for each wing plan form are presented about a point in the chord plane of the wing at the quarter chord of the mean aerodynamic chord. The mean aerodynamic chord and the wing area used to reduce the results to coefficients are those for each wing plan form.

The coefficients and symbols used in this paper are defined as follows:

C_L	lift coefficient, $\frac{\text{Lift}}{qS}$
C_m	pitching-moment coefficient, $\frac{\text{Pitching moment}}{qS\bar{c}}$
C_D	drag coefficient, $\frac{\text{Drag}}{qS}$
C_Y	side-force coefficient, $\frac{\text{Side force}}{qS}$
C_n	yawing-moment coefficient, $\frac{\text{Yawing moment}}{qSb}$
C_l	rolling-moment coefficient, $\frac{\text{Rolling moment}}{qSb}$
C_{D_i}	duct internal-drag coefficient, $\frac{\text{Internal drag}}{qS}$
C_{D_c}	chamber-drag coefficient, $\frac{\text{Chamber drag}}{qS}$

C_{D_b}	base-drag coefficient, $\frac{\text{Base drag}}{qS}$
C_{L_α}	lift-curve slope
$C_{m_{C_L}}$	pitching-moment-curve slope
L/D	lift-drag ratio
$\frac{\Delta C_D}{{C_L}^2}$	drag-due-to-lift factor, $\frac{C_D - C_{D_{min}}}{{C_L}^2}$
M	Mach number
q	free-stream dynamic pressure, $0.7pM^2$, lb/sq ft
p	free-stream static pressure, lb/sq ft
R	Reynolds number
S	wing area, sq ft
c	local chord, ft
$\bar{c}$	wing mean aerodynamic chord, ft
b	wing span, ft
X, Y, Z	stability axes (see fig. 1)
α	angle of attack of fuselage reference line, deg
β	angle of sideslip, deg
$\Lambda_{c/4}$	sweepback of quarter-chord line, deg
θ	test-section flow angle, deg

Subscripts:

max	maximum
min	minimum

MODEL AND APPARATUS

Details of the wing-fuselage combinations are shown in figure 2. Details of the tail configuration are shown in figure 3. The geometric characteristics of the model are given in table I. Photographs of the model mounted in the test section of the Langley Unitary Plan wind tunnel are given in figure 4.

The fuselage of the model had a fineness ratio of 16.18 not including the model ducts. The aspect ratio of each wing plan form was 3.20. One wing plan form had the quarter-chord line swept back 45.0°, a taper ratio of 0.20, and NACA 64A204.5 airfoil sections. The other wing had the quarter-chord line swept back 19.2°, a taper ratio of 0.40, and 3.5-percent-thick circular-arc airfoil sections. Both wings were equipped with tip-mounted external stores. The tail configuration consisted of a 50.0° sweptback vertical tail with a 40.0° sweptback horizontal tail located at the tip of the vertical tail. The horizontal tail had 15.0° of dihedral.

The model had ducts mounted on each side of the fuselage. The inlets were of the two-dimensional type and were equipped with boundary-layer diverters that were approximately 1/8 inch in height. The ducts discharged air through circular exits at the fuselage base on each side of the fuselage.

The tests were conducted in the low Mach number test section of the Langley Unitary Plan wind tunnel. This tunnel is a variable-pressure, continuous, return-flow type. The test section is 4 feet square and approximately 7 feet in length. The nozzle leading to the test section is of the asymmetric sliding-block type and variable Mach numbers may be obtained continuously through a Mach number range from approximately 1.57 to 2.87 without tunnel shutdown.

Forces and moments on the model were measured by a six-component internal strain-gage balance. The balance was attached, by means of a model sting, to the tunnel central support system.

Changes in the model attitude were accomplished by an angular positioning of the central support system in the horizontal plane. Variable-angle-of-attack tests were made with the wing of the model in the vertical plane. Variable-angle-of-sideslip tests were made with the wing in the horizontal plane.

The pressure at the base of the model and in the chamber housing the internal balance was measured by pressure-sensitive electrical pick-ups. The pressures in the ducts were indicated by deflection of liquid in a conventional manometer board. One duct was instrumented with a rake consisting of four total-pressure tubes 90° apart and two static-pressure tubes. The total- and static-pressure measurements were taken in a plane perpendicular to the exit center line and 1/2 inch upstream of the exit. The other duct was instrumented with one total-pressure tube located on the center line of the exit. This duct was fitted with a plate-type choke ring at the duct exit to assure the formation of a normal shock. The total pressure was measured 1/16 inch upstream of the front face of the choke ring.

TESTS

Tests were made through an angle-of-attack range from about -8° to about 10° at an angle of sideslip of approximately 0° on the wing-fuselage combination at Mach numbers of 1.79, 1.89, 1.99, 2.18, and 2.67. Tests were also made at various Mach numbers at an angle of attack of -2.5° and an angle of sideslip of approximately 0°. One run was made through an angle-of-sideslip range from -5.0° to 5.0° at an angle of attack of -2.5°.

Tests were limited in some instances due to reflected wave interference with the model and also due to the strength of the model and model sting. The strength of the model and model sting required limiting the maximum angle of attack at $M = 2.67$ to about 5°. The reflection of the fuselage-nose compression shock interfered with the external store on the 45.0° swept-wing model at Mach numbers less than about 1.8 at an angle of sideslip of 0°. A Mach number of 2.18 was the minimum Mach number at which the store was reflection free throughout a practical range of sideslip angles. Hence, the determination of the complete-model lateral stability characteristics was made at $M = 2.18$ over a range of angles of sideslip from -5° to 5°.

The test conditions are summarized in the following table:

M	q, lb/sq ft abs	R for -	
		19.2° swept wing	45.0° swept wing
1.69	683	2.46×10^6	
1.79	665	2.34	2.60×10^6
1.89	638	2.25	2.50
1.99	606	2.16	2.39
2.08	574	2.07	2.30
2.18	533	1.98	2.19
2.67	456	1.54	1.71

The stagnation pressure was 12.0 pounds per square inch absolute for all tests.

CORRECTIONS AND ACCURACY

Inasmuch as the calibration of the test section had not been completed at the time the data were taken, no corrections have been applied for stream angularity or buoyancy. However, it has been found that longitudinal pressure gradients are so small as to have a negligible buoyancy effect on the model. A preliminary evalution of the calibration of air-flow angularity indicates that angularity exists only in the vertical plane of the test section. Since both pitch and sideslip tests were made with the model wings in the vertical plane, no correction of the plotted results presented herein is required to account for stream angularity. The approximate values of flow angularity in the vertical plane of the test section are given in the following table:

M	θ, deg
1.79	0.4
1.89	.7
1.99	.9
2.18	1.3
2.67	.6

The flow angle is in a direction to increase positively the sideslip angles for pitch tests and the angles of attack for sideslip tests.

The maximum deviation of local Mach number in the part of the tunnel occupied by the model was ±0.015. The angles of attack and sideslip have been corrected for the deflection of the support system under load.

The drag coefficients presented have had subtracted from them the base- and chamber-drag coefficients. This results in net model drag coefficients which have a static pressure at the model base and in the balance chamber equal to free-stream static pressure.

The internal-drag coefficient has not been subtracted from the total measured drag coefficient. In order to obtain external-drag coefficients, it is necessary to subtract the internal-drag coefficients from the model drag coefficients presented.

The internal-drag coefficients were calculated from the six-tube rake pressure measurements. The internal-drag coefficients computed from the measured total pressure in front of the ring choke were in excellent agreement with the rake values.

PRESENTATION OF RESULTS

The results of this investigation are presented in the following figures:

Figure

Internal-, base-, and chamber-drag coefficients 5
Schlieren photographs of the model with the 19.2° swept wing 6
Schlieren photographs of the model with the 45.0° swept wing 7
Aerodynamic characteristics in pitch 8
Variation of longitudinal aerodynamic characteristics with Mach number 9
Aerodynamic characteristics in sideslip 10
Summary of the longitudinal aerodynamic characteristics with Mach number 11

RESULTS

The results of this investigation are presented without analysis. It is pertinent, however, to make several observations with regard to what is shown by the data:

(1) The lift-curve slope of the model with 19.2° swept wing is higher than that for the 45.0° swept wing and the minimum drag coefficient is about 0.0040 lower than that for the 45.0° swept-wing model probably due to the thinner wing section. The drag-due-to-lift factor is essentially the same for both wing plan forms.

(2) The aerodynamic center is from 10 to 12 percent of the mean aerodynamic chord farther rearward on the model with the 45.0° swept wing than on the model with the 19.2° swept wing.

(3) The model with the 19.2° swept wing and the complete tail, the only configuration on which lateral stability results were obtained, is directionally stable for the test conditions (Mach number of 2.18 and an angle of attack of -2.5°).

Langley Aeronautical Laboratory,
National Advisory Committee for Aeronautics,
Langley Field, Va., March 10, 1958.

[redacted]

TABLE I.- PHYSICAL CHARACTERISTICS OF THE TEST MODEL

	Wing		Tail	
	45.0° Sweptback	19.2° Sweptback	Horizontal	Vertical
Area, sq ft	1.822	1.742	0.354	0.292
Span, in.	28.980	28.328	13.320	6.480
Aspect ratio	3.20	3.20	3.50	1.00
Taper ratio	0.20	0.40	0.30	0.67
Sweep of quarter chord, deg . . .	45.0	19.20	40.0	50.0
Airfoil section	NACA 64A204.5	3.5-percent circular-arc	NACA 64A005	NACA 64A007
Incidence angle with respect to fuselage reference line, deg:				
Root	2.0	2.0	-2.0	
Theoretical tip	-2.0	2.0	-2.0	
Dihedral angle, deg	-4	0	15.0	
Mean aerodynamic chord, in. . . .	10.414	9.395	9.366	6.562
[a]Tail length, ft:				
45.0° sweptback wing			2.011	1.463
19.2° sweptback wing			1.944	1.396

[a]Tail length is the distance from the $\bar{c}/4$ of the wing to the $\bar{c}/4$ of the tail component.

[redacted]

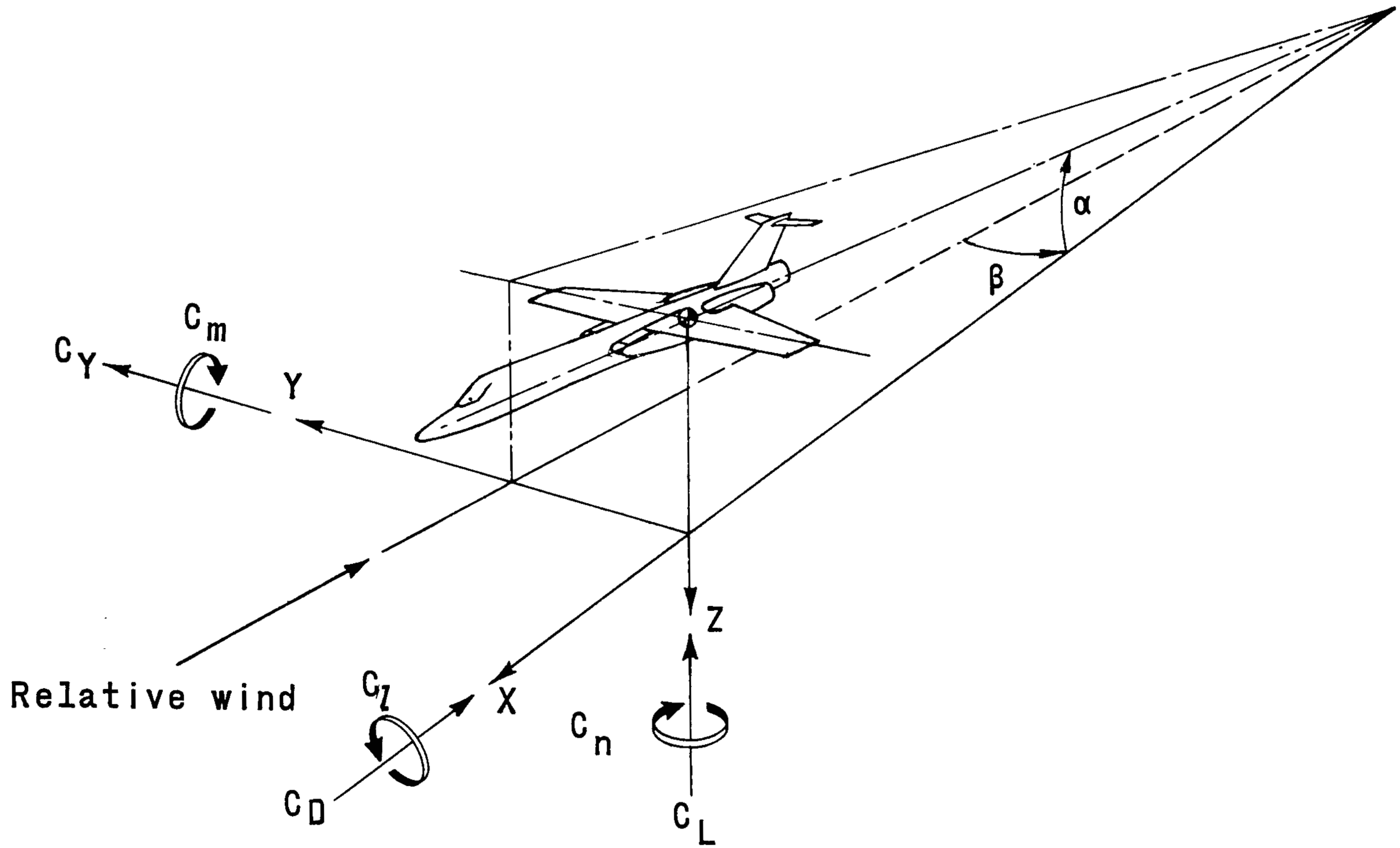

Figure 1.- Stability system of axes. Positive values of forces, moments, and angles are indicated by arrows.

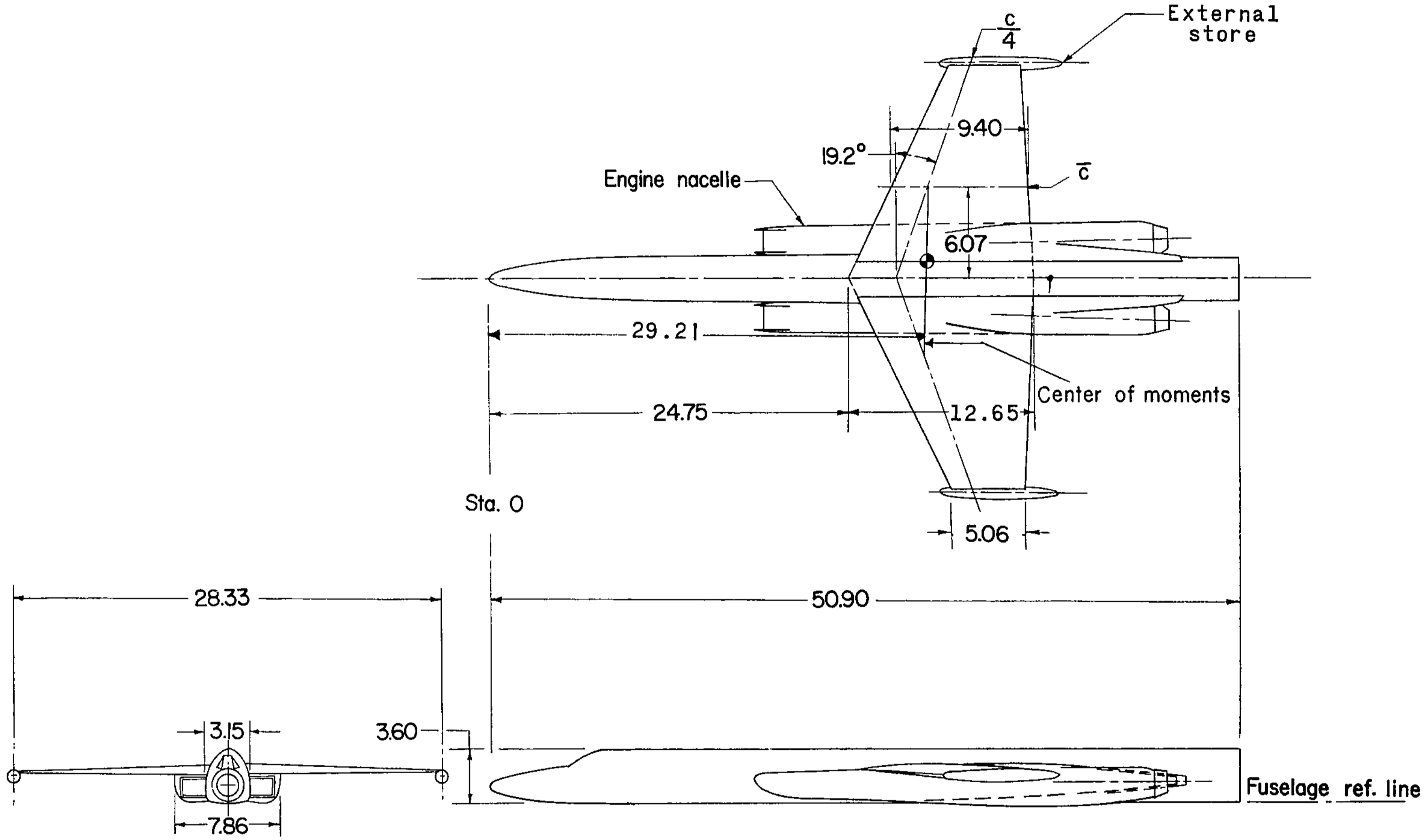

(a) $\Lambda_{c/4} = 19.2^{\circ}$.

Figure 2.- Three-view sketch of the test model.

~~CONFIDENTIAL~~

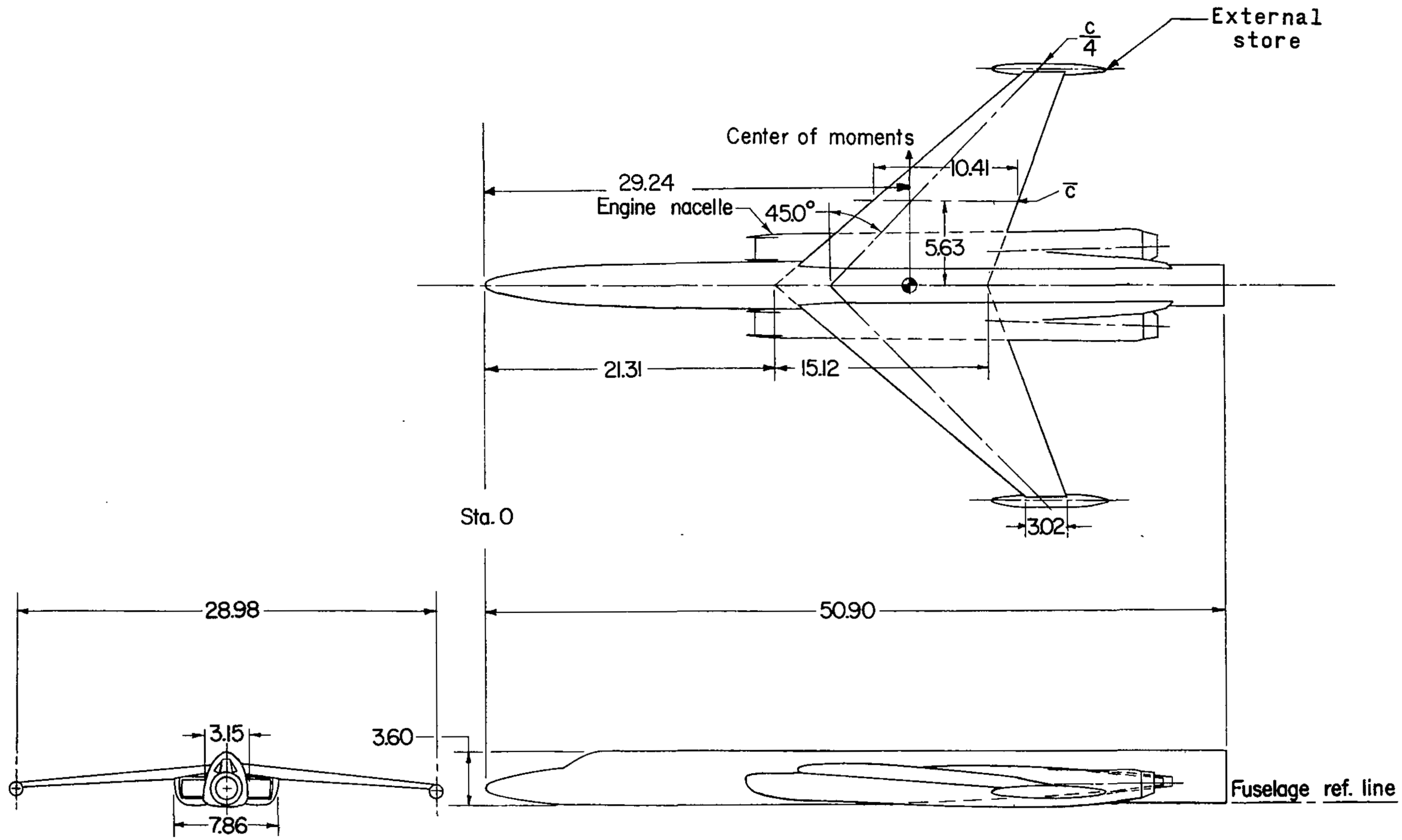

(b) $\Lambda_{c/4} = 45.0^{\circ}$.

Figure 2.- Concluded.

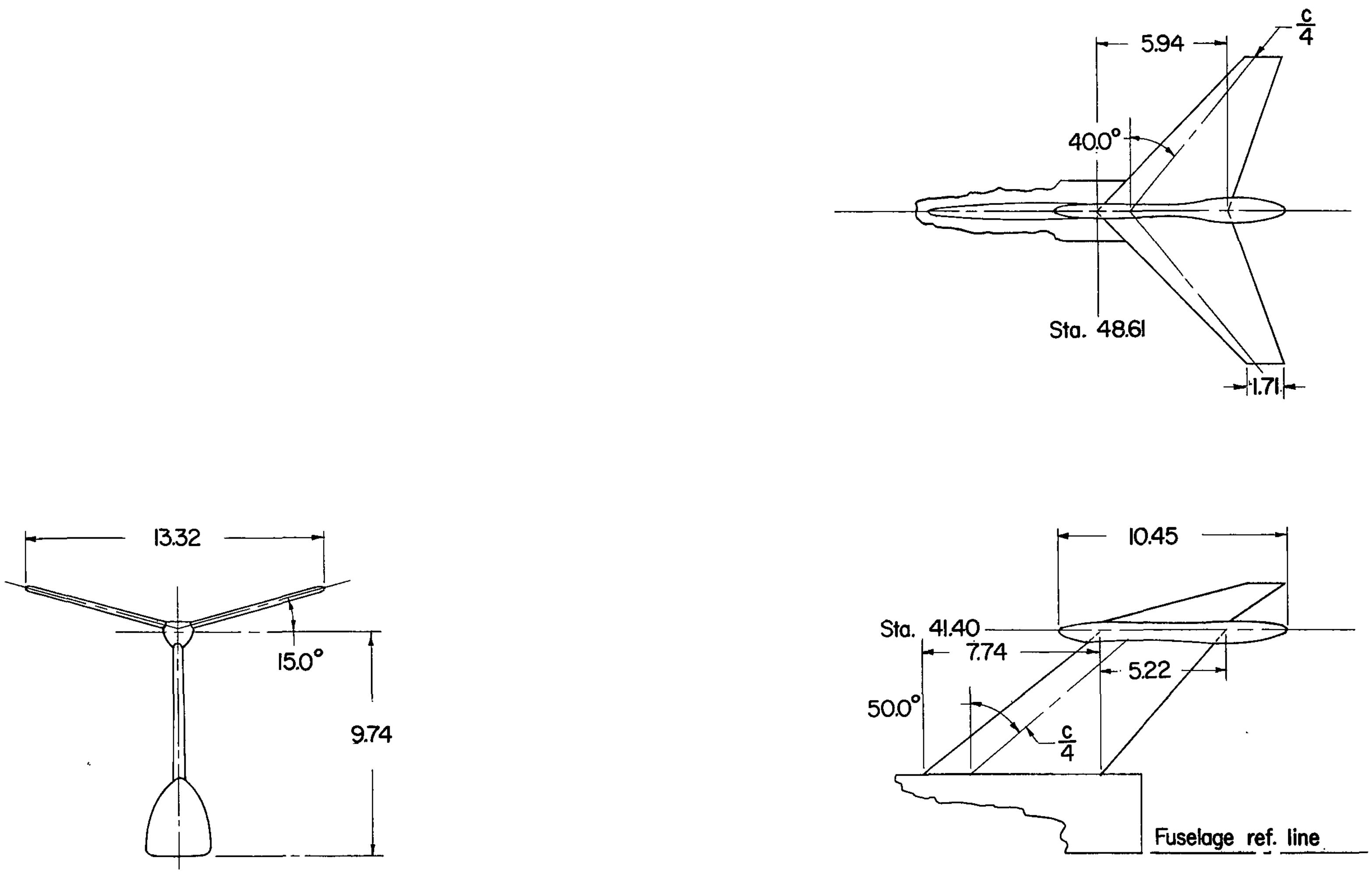

Figure 3.- Drawing showing the arrangement of the vertical and horizontal tails on the test model.

[redacted]

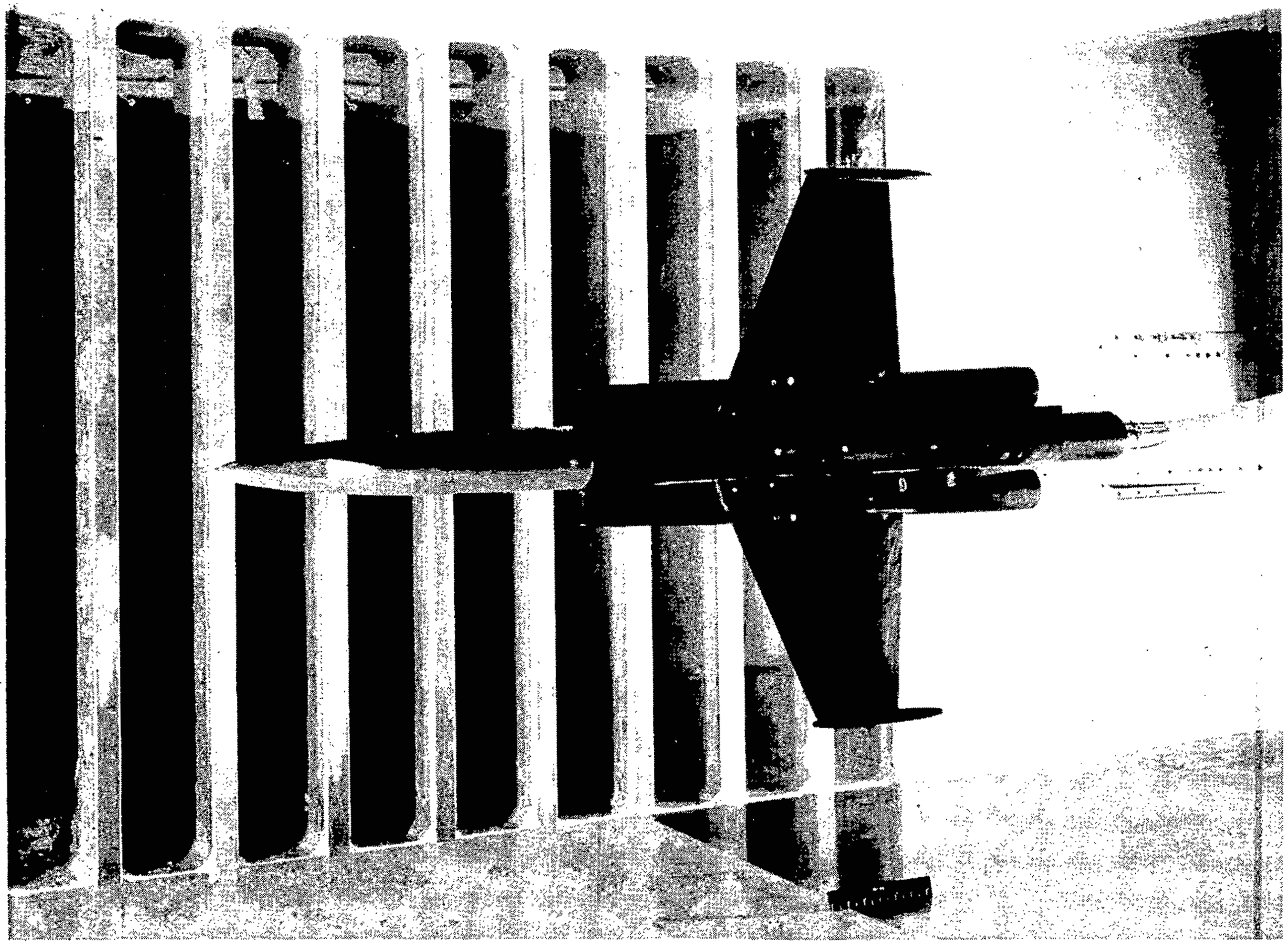

(a) $\Lambda_{c/4} = 19.2^{\circ}$. L-92204

Figure 4.- Photographs of the test model in the Langley Unitary Plan wind tunnel.

[redacted]

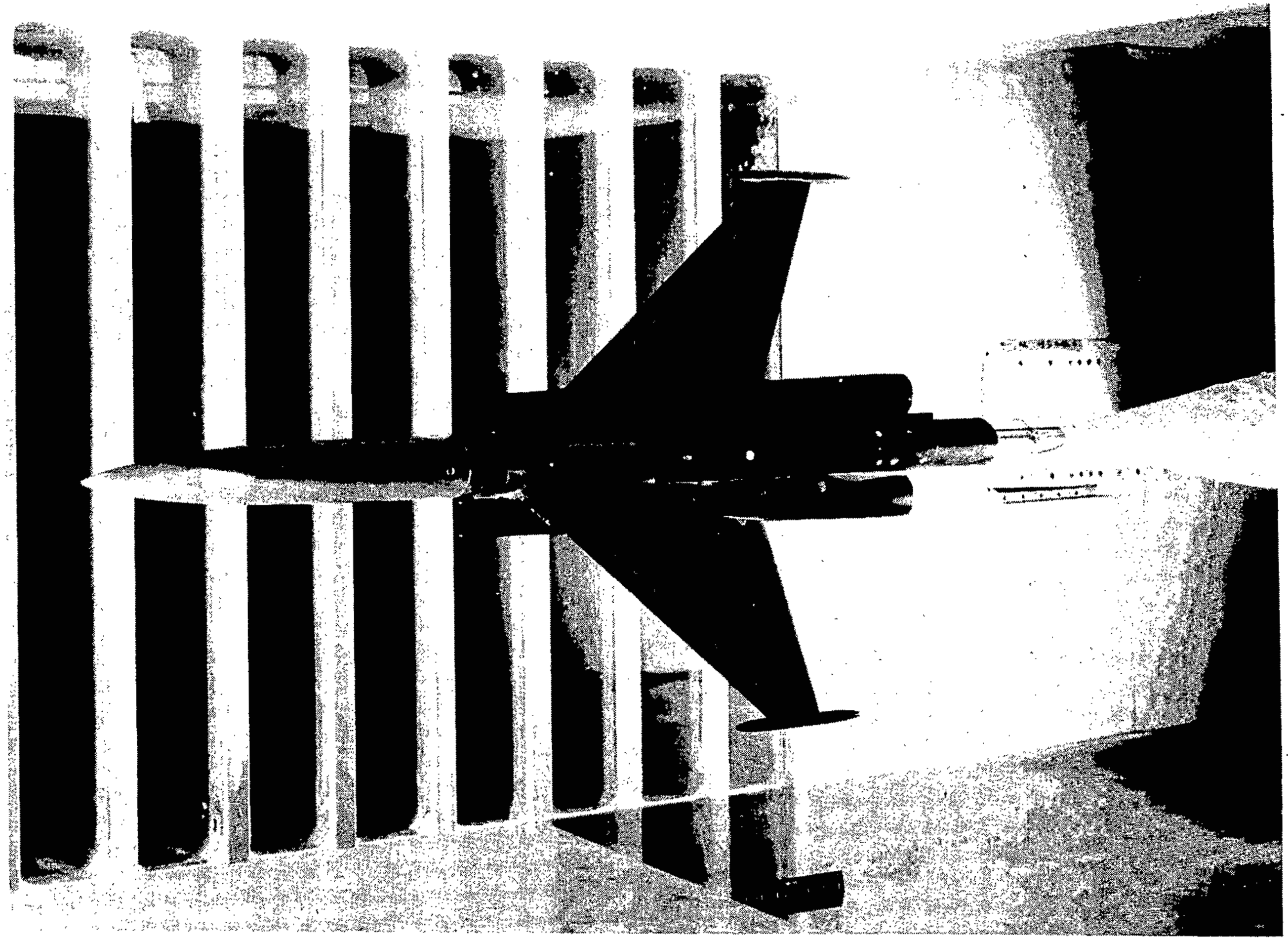

(b) $\Lambda_{c/4} = 45.0^{\circ}$. L-92202

Figure 4.- Concluded.

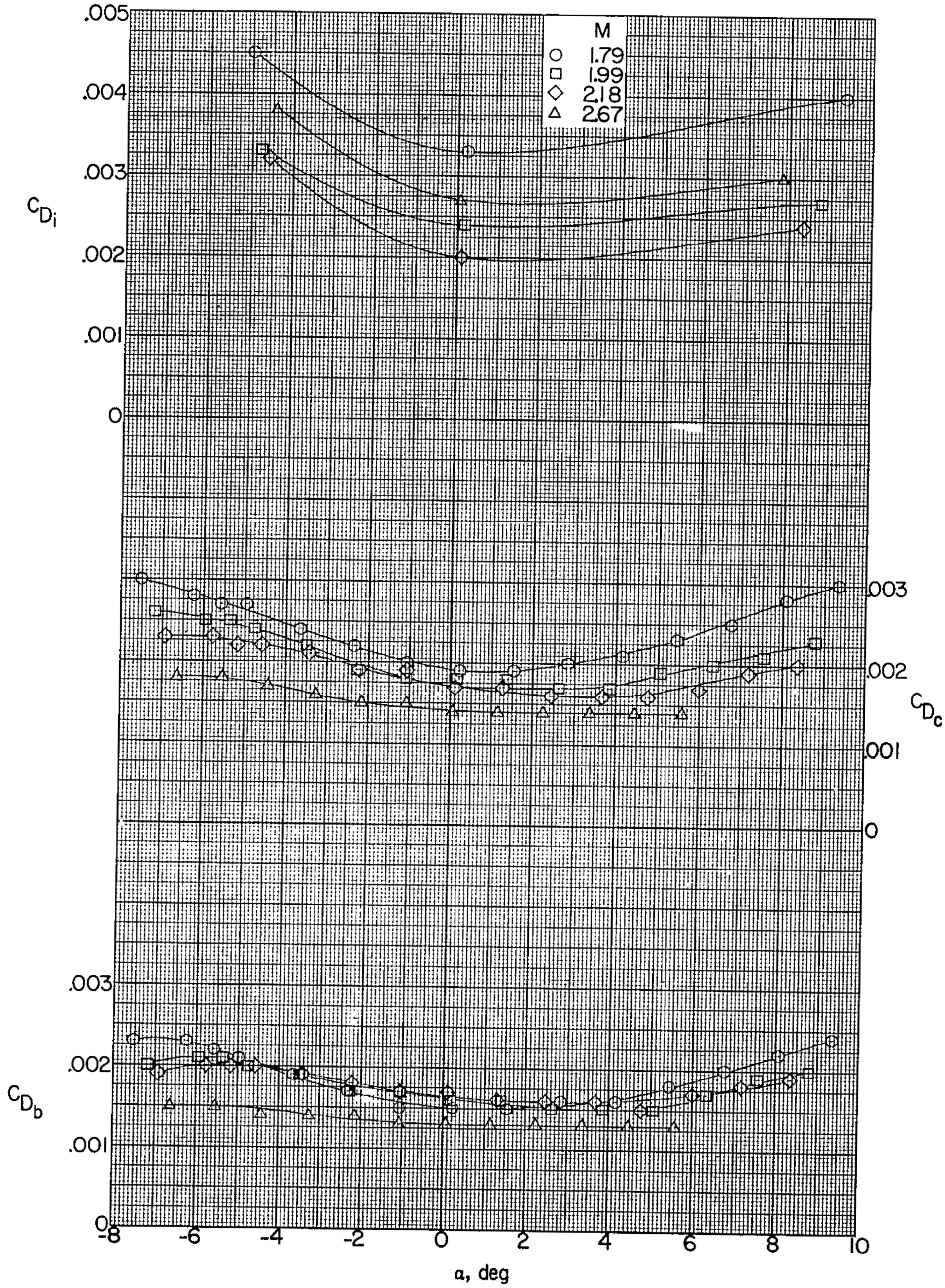

(a) $\Lambda_{c/4} = 19.2^{\circ}$.

Figure 5.- Variation of internal-, base-, and chamber-drag coefficients with angle of attack of the model without tail. $\beta = 0.3^{\circ}$.

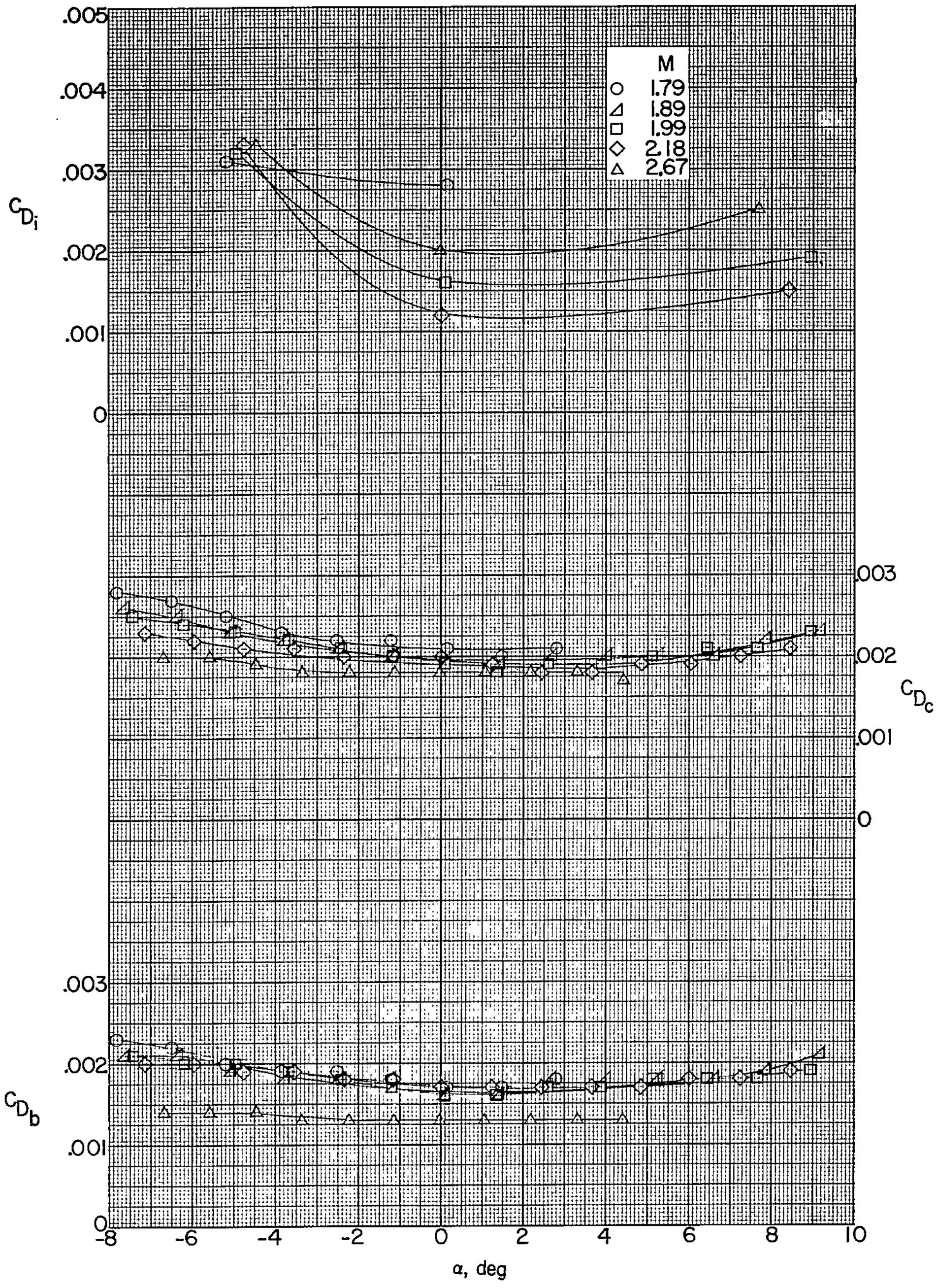

(b) $\Lambda_{c/4} = 45.0^{\circ}$.

Figure 5.- Concluded.

[redacted]

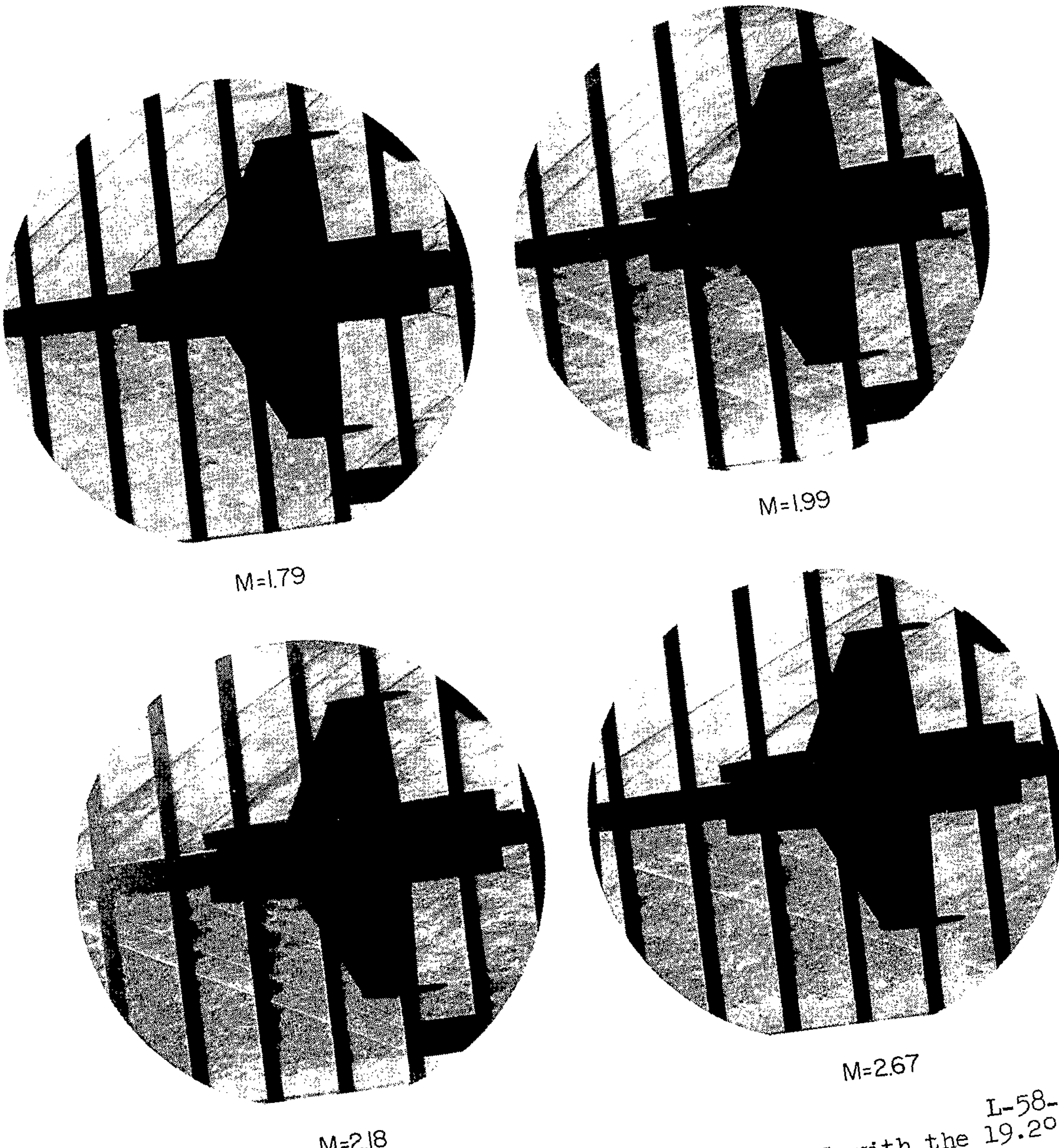

L-58-161

Figure 6.- Schlieren photographs of the test model with the 19.2° of sweptback wing. $\alpha \approx 0^{\circ}$; $\beta = 0.3^{\circ}$.

[redacted]

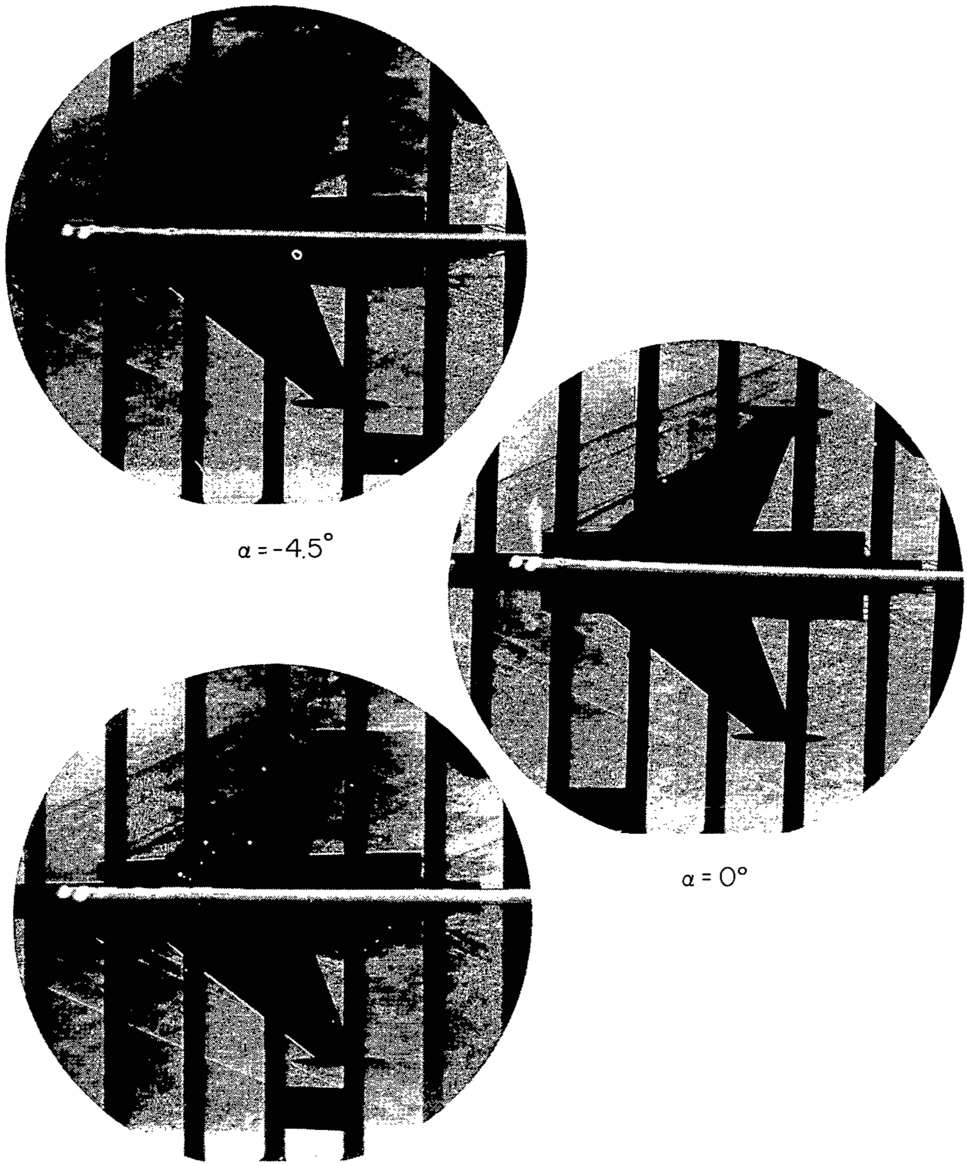

L-58-162

Figure 7.- Schlieren photographs of the test model with the 45.0° of sweptback wing at a Mach number of 2.67.

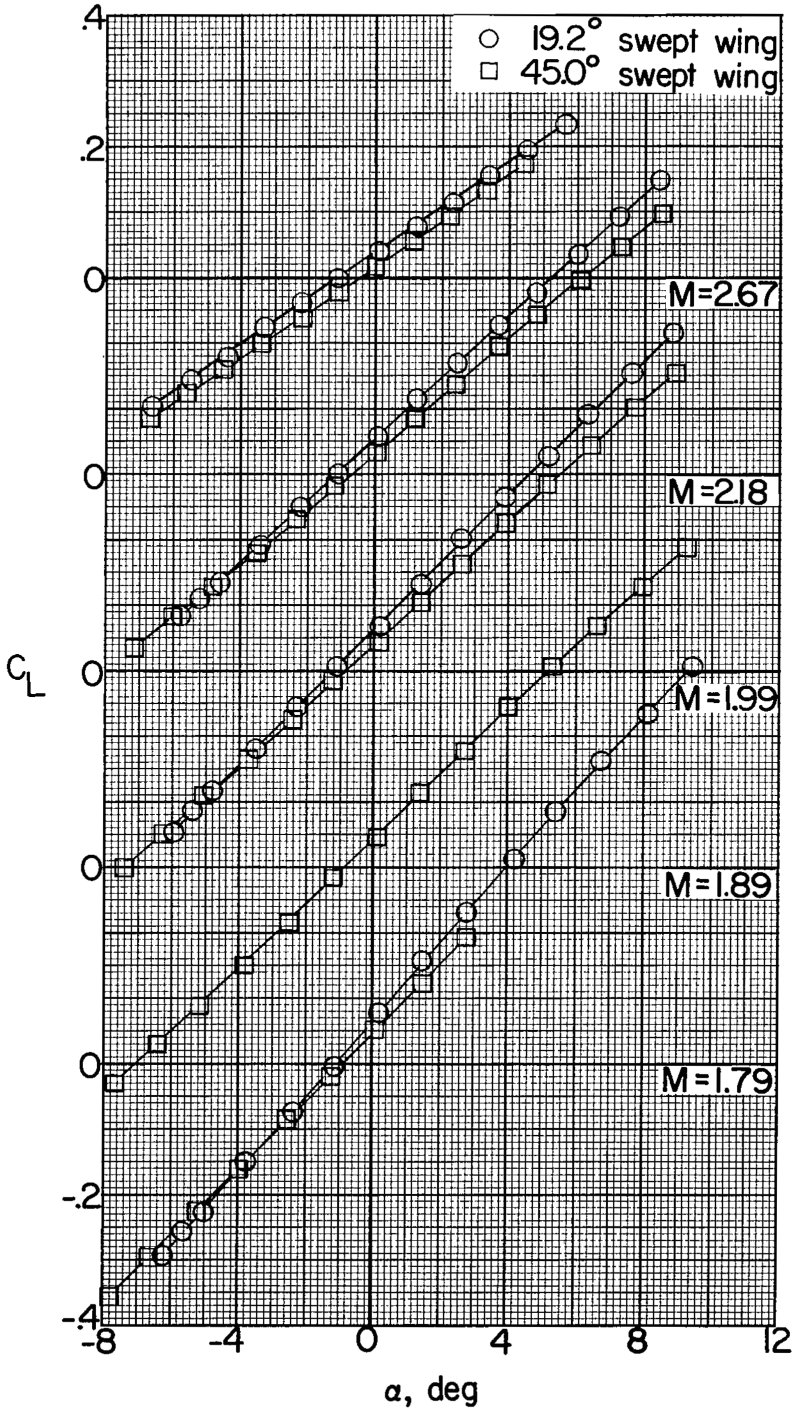

Figure 8.- Aerodynamic characteristics in pitch of the test model without tail and with two wing plan forms. $\beta = 0.3^\circ$.

[redacted]

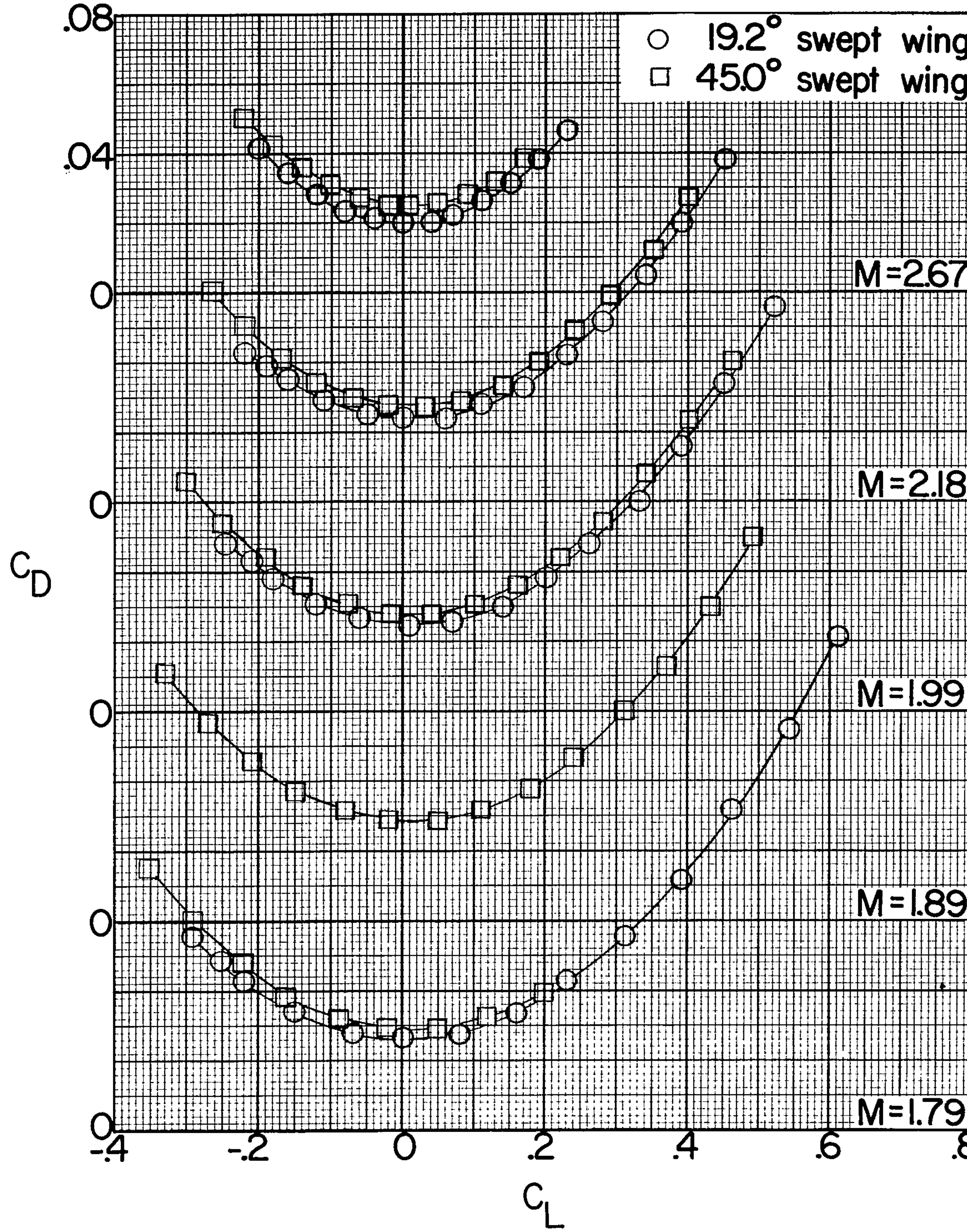

Figure 8.- Continued.

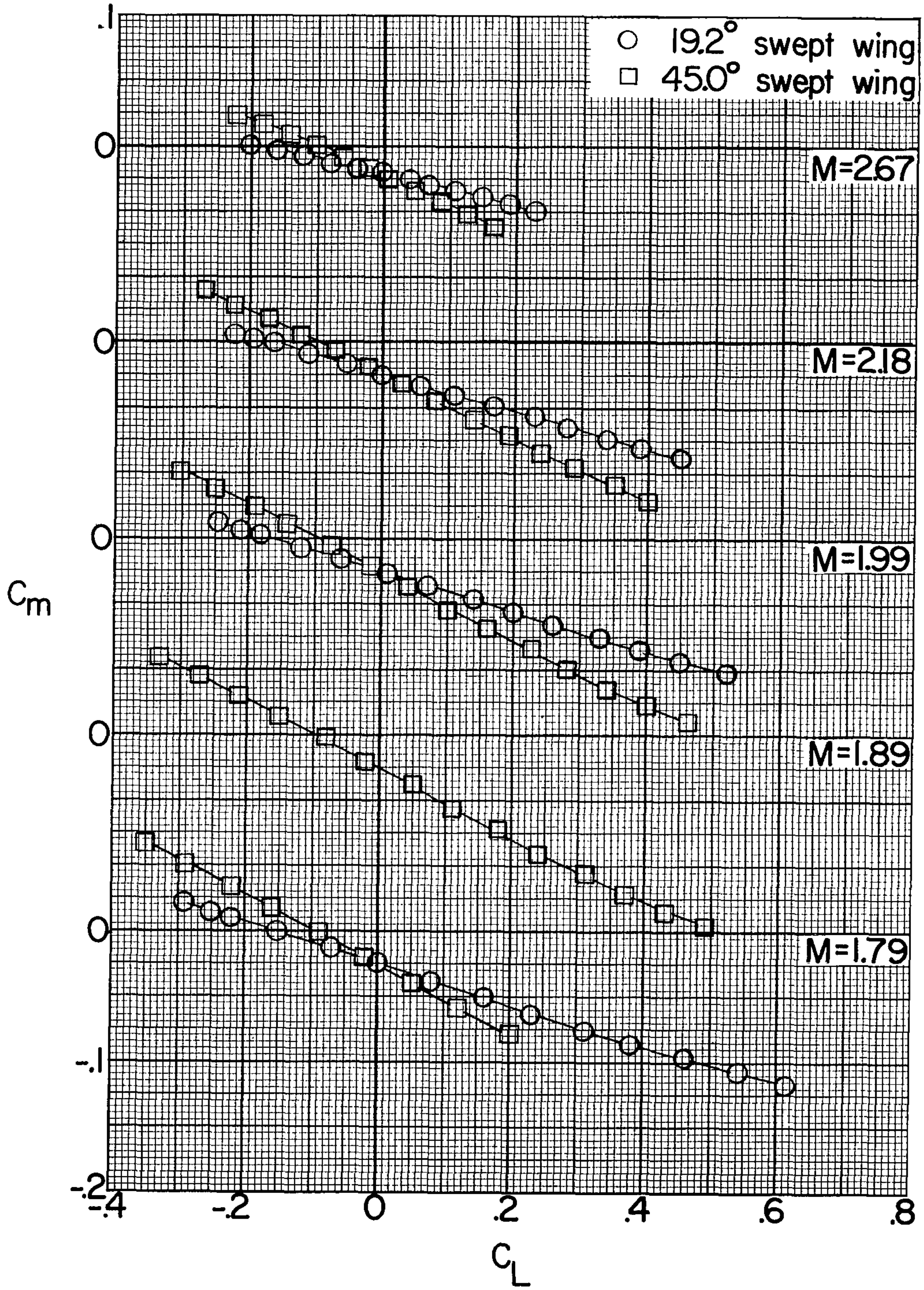

Figure 8.- Concluded.

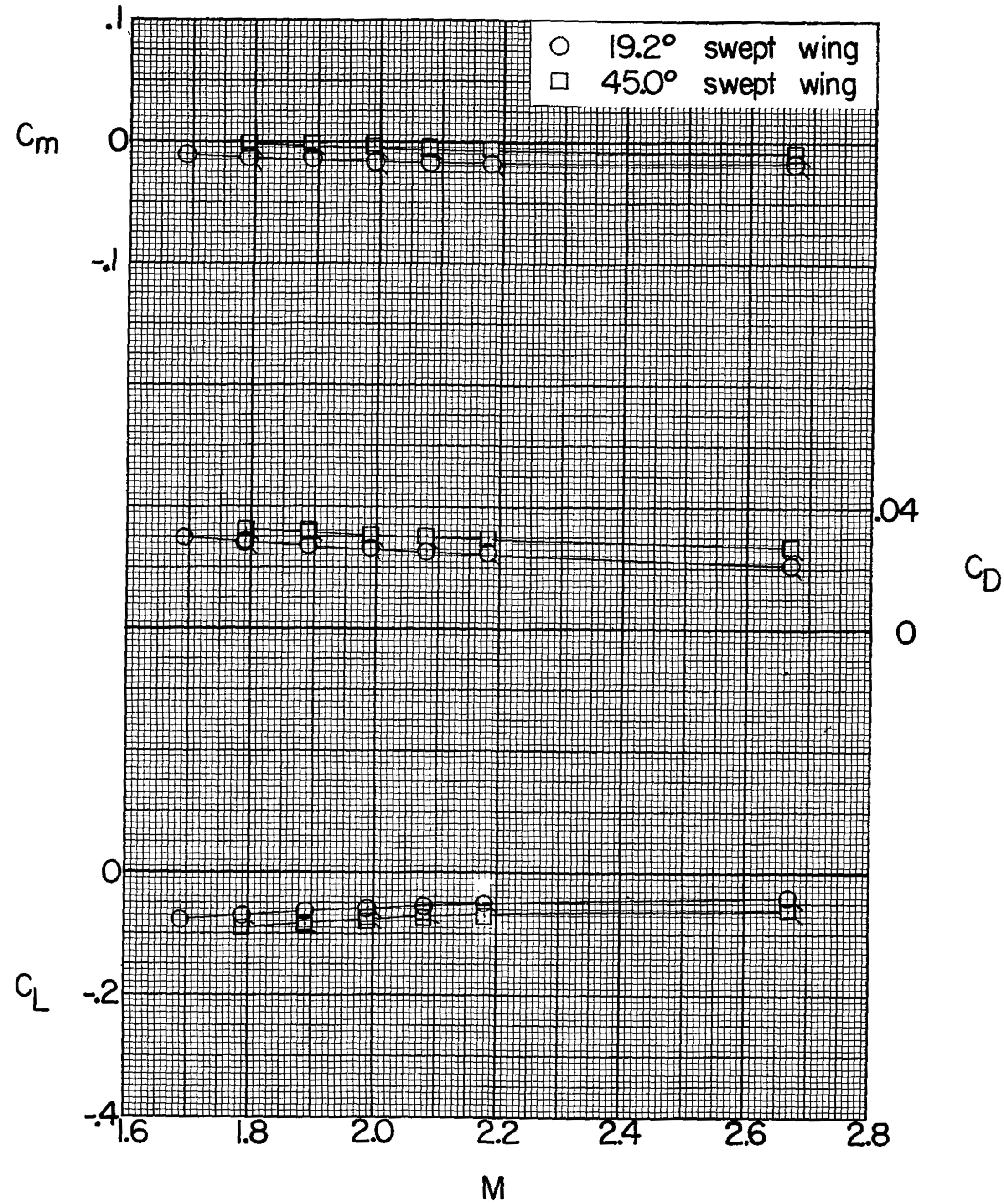

Figure 9.- Longitudinal characteristics of the test model without tail and with two wing plan forms at several Mach numbers. $\alpha = -2.5^{\circ}$; $\beta = 0.3^{\circ}$. (Flagged symbols were obtained from the results of fig. 8.)

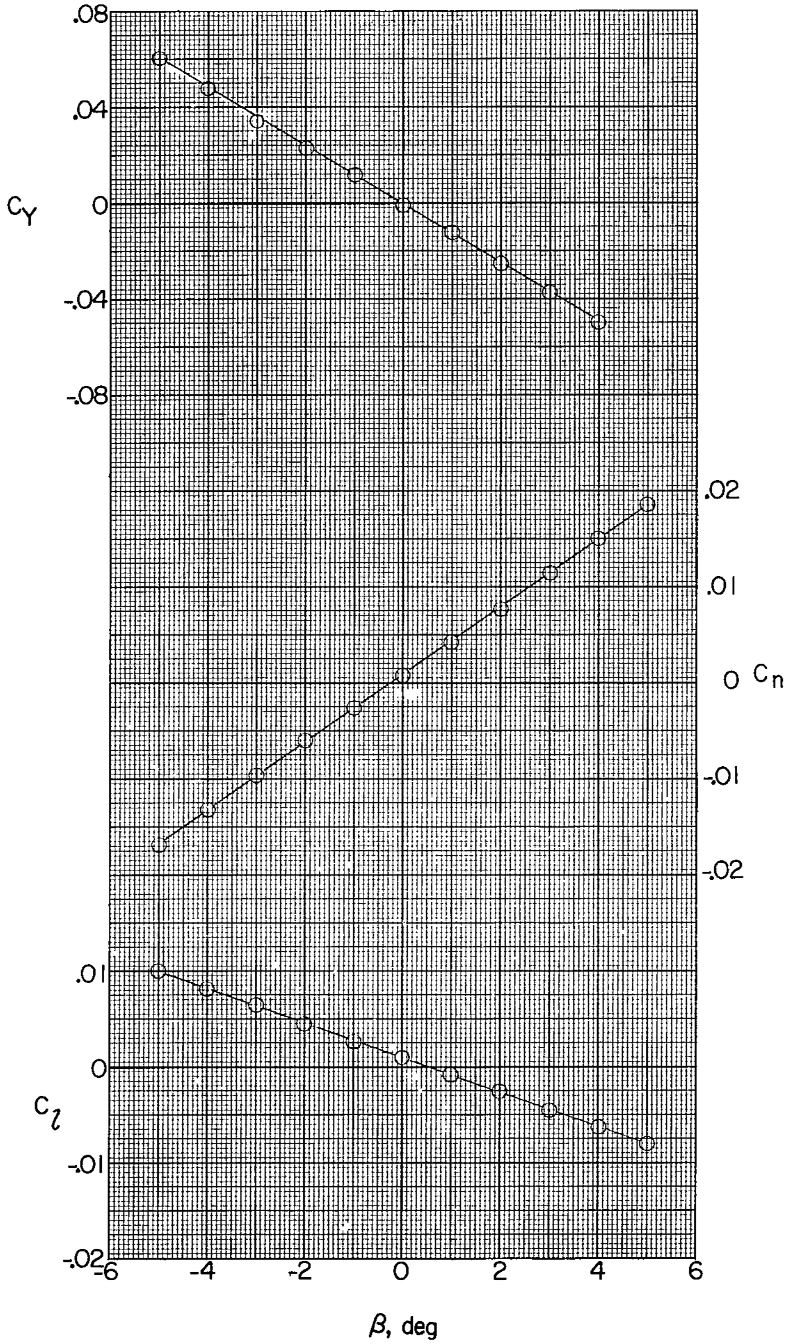

Figure 10.- Aerodynamic characteristics in sideslip of the test model with tail and with the 19.2° sweptback wing at $M = 2.18$. $\alpha = -2.5°$; $C_L = 0.10$.

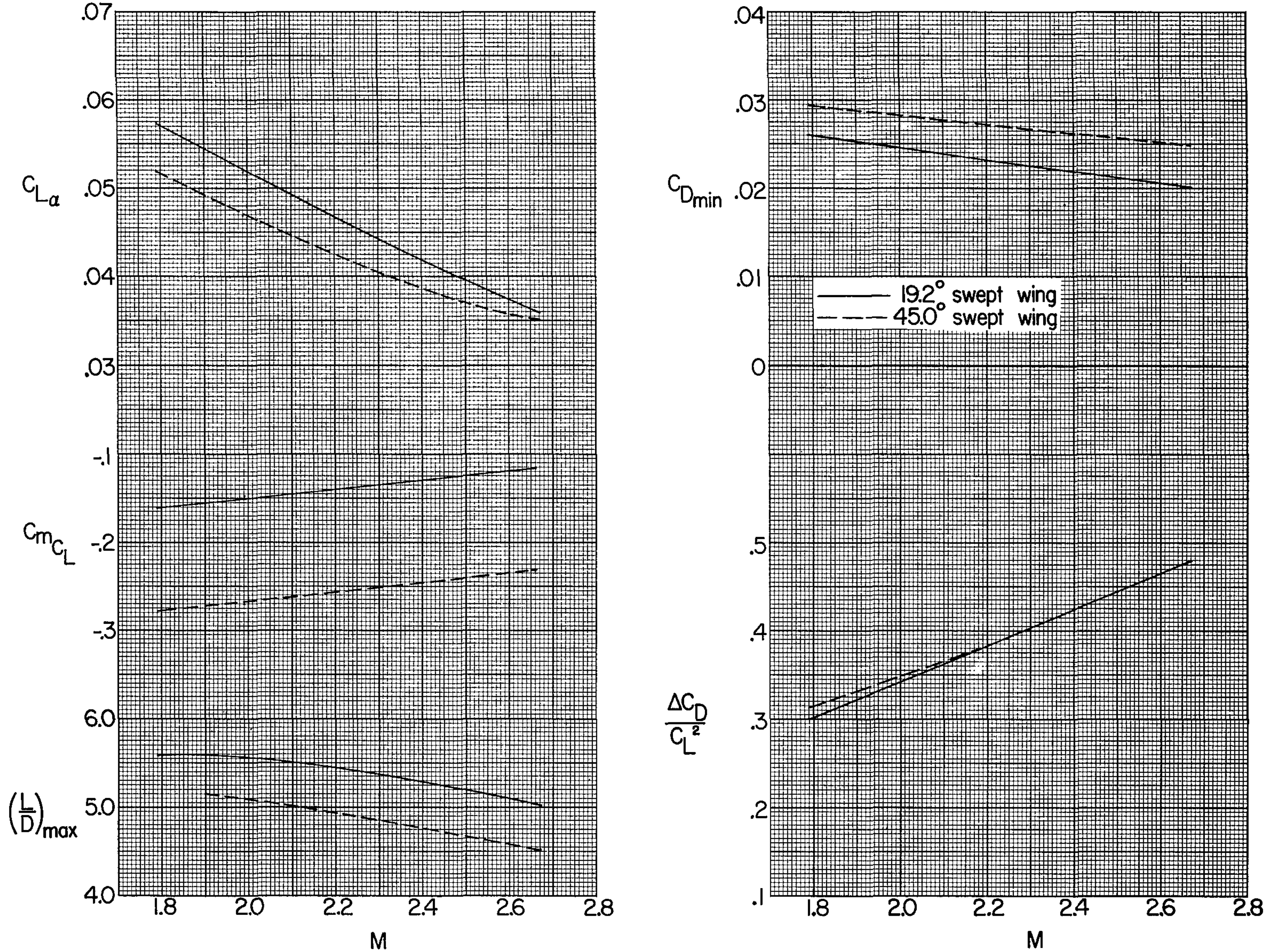

Figure 11.- Summary of the longitudinal aerodynamic characteristics of the test model without tail.